Colloids and Surfaces A: Physicochemical and Engineering Aspects 613 (2021) 126061

Contents lists available at ScienceDirect

Colloids and Surfaces A: Physicochemical and Engineering Aspects

journal homepage: www.elsevier.com/locate/colsurfa

Antioxidant and hydrophobic Cotton fabric resisting accelerated ageing

Giulia Mazzon [a,b,*], Marco Contardi [a], Ana Quilez-Molina [a], Muhammad Zahid [a], Elisabetta Zendri [b], Athanassia Athanassiou [a], Ilker S. Bayer [a,*]

[a] Smart Materials, Istituto Italiano di Tecnologia, via Morego, 30, 16163, Genova, Italy
[b] Dipartimento di Scienze Ambientali, Informatica e Statistica (DAIS), Università Ca' Foscari Venezia, Via Torino 155, 30172, Venice Mestre, Italy

GRAPHICAL ABSTRACT

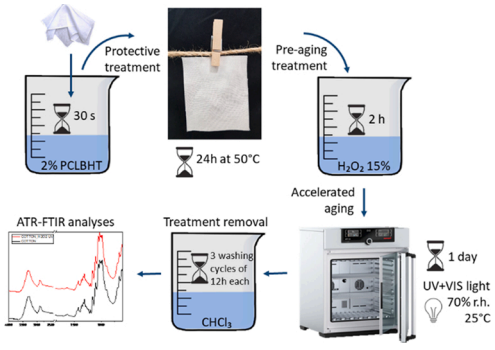

ARTICLE INFO

Keywords:
Cotton
Antioxidant fabric
Hydrophobic fabric
Ageing
Ecofriendly

ABSTRACT

Antioxidant fabrics are excellent shields against oxidative damage by free radicals and can be used in clothing, packaging, cosmetics and preservation. In this study, we developed antioxidant and hydrophobic cotton fabrics using ecofriendly materials and processes. The fabrics were functionalized with a double layer coating. Pristine cotton fabrics were coated with a food grade antioxidant (butylated hydroxytoluene, BHT) incorporated biodegradable polyester (polycaprolactone, PCL). This coating was shielded with an acetoxy functional biocompatible hydrophobic silicone coating. The hydrophobic shielding prevented potential loss of the antioxidant due to interaction with water or ambient humidity over time. Coated fabrics were exposed to extreme peroxidative (concentrated H_2O_2) and UV light damage conditions using an *ad hoc* protocol for simulating decades of atmospheric ageing. Chemical changes on the cotton surface and potential oxidation and preventive mechanisms were studied using spectroscopy. Treated fabrics also displayed very low water vapor uptake and remained breathable with no visible color change. Mechanical properties of the original fabric were preserved after the treatment.

* Corresponding authors at: Smart Materials, Istituto Italiano di Tecnologia, via Morego, 30, 16163, Genova, Italy.
E-mail addresses: Giulia.mazzon@iit.it (G. Mazzon), ilker.bayer@iit.it (I.S. Bayer).

https://doi.org/10.1016/j.colsurfa.2020.126061
Received 26 October 2020; Received in revised form 2 December 2020; Accepted 14 December 2020
Available online 30 December 2020

1. Introduction

The preservation of textiles from deterioration is a major issue for conservators and conservation scientists, considering that the category "textiles" includes valuable canvases, carpets, tapestries, curtains, costumes, design objects [1,2]. The preservation of the aforementioned objects is of fundamental importance in cultural heritage. Deterioration of these textiles is primarily governed by the presence of humidity [3–5]. Rapid variations in humidity can cause swelling or shrinkage of cellulose fibers, that are among the principal constituents of the ancient textiles [6], resulting in irreversible tensions, especially when occurring in large artworks or objects [7]. Furthermore, in presence of humidity, the air contaminants SO_2, NO_2, and CO_2 can turn into sulfuric, nitric, and carbonic acids, respectively [8]. Cellulose can react with these acids at room temperature, triggering a hydrolysis process inside the polysaccharide chains, that leads to the scission of original cellulose structures, making the textile less resistant [9–11]. Constant exposure to high humidity can also promote microbial/bacterial growth and proliferation [12–14]. When insects and microorganisms attack a textile, they rapidly degrade it through enzymatic reactions by releasing excrements [15, 16]. Hence, humidity has a significant impact on the conservation of artworks [17,18].

Besides humidity, oxidative degradation with ambient light and oxygen (oxidation) [19] is another source of textile deterioration. Experiments demonstrated that fabric samples stored in dark conditions suffered less strength loss compared to others exposed to light [20,21]. However, long periods of storage in the dark is not a viable option for public display and museum profitability. As such, textile preservation against stresses induced by oxidative processes and humidity [22] should involve the use of protective coatings to significantly reduce the diffusion of harmful oxidative peroxide radicals into the fabric. An ideal protective coating should confer hydrophobicity, reduce absorption of ambient moisture and maintain the breathability of the original fabric to prevent humidity accumulation and development of the microorganisms [23–25]. Moreover, it should be transparent, conformal to the textile structure without altering its texture, maintain or improve mechanical properties, and interact with the textile in a non-intrusive way [26,27]. In the past, several polymeric coatings based on acrylic copolymers [28–31], polydimethylsiloxane [32–35] and polymeric composites with nanoparticles [36–39] have been developed for conservation purposes. Due to ecological issues related to fluorinated coatings (C-8 chemistry was expelled by Environmental Protection Agency due to health risks [40]), research on fluorine-free protective coatings has accelerated recently [41–45]. These coatings are usually integrated with active substances such as UV absorbers, antioxidants or oxidizing agent quenchers to minimize the deterioration of the textiles, as summarized by Koussoulou [46]. Antioxidant treatment was applied for conservation purposes by Hackney et al. [20], based on commercial antioxidants: Irganox 1010, Irganox 565, and Topanol CA. Authors observed that 1% wt. concentration produced little visual change, whereas the 2% wt. antioxidant additions resulted in an opaque to white coating. Antioxidant, antibacterial, and UV-resistant properties were successfully tested on not historical fabrics treated with CuO nanoparticles by Altun and Becenen [47]. A colorless and chemically stable solution based on hexamethyltriethylene tetramine and $Zn(NO_3)\cdot 6H_2O$ has been applied onto cotton fabrics by Shaheen et al. [48] conferring an antibacterial and UV protective function.

Some other studies provided protective treatments against photodegradation and water uptake-induced deterioration. Hou et al. [49] developed a robust polyhedral oligomeric silsesquioxanes (POSS)- based superhydrophobic treatment, which resulted in fabrics with a water contact angle of 159° with resistance to UV irradiation, high-temperature exposure, ultrasonic washing, and mechanical abrasion. Abd El-Hady et al. [50] coated cotton fabrics by developing multilayers of poly(diallyldimethylammonium chloride), ZnO/SiO_2 colloidal solution nanocomposite, and stearic acid. The multilayers conferred UV protection properties to the cotton fabric and improved water repellency. A silica coating on the fabrics was produced by Parhizkar et al. [51] using UV stabilizers, modifying the surface wettability and conferring to the fabrics high abrasion durability and acceptable wash fastness. In another work, cotton fabric with photochromic, hydrophobic, antibacterial, and ultraviolet (UV) blocking properties was developed by Ayazi-Yazdi et al. [52] with a mixture of silica nanoparticles, spirooxazine as a photochromic dye and an alkylsilane compound. Photo-stability in an accelerated ageing environment of a protective acrylic coating and the influence of rutile-TiO_2 nanoparticles along with an amine light stabilizer (HALS) have been quantitatively studied by monitoring the chemical modifications occurring upon ageing conditions by Nguyen et al. [53]. Note that in all the aforementioned studies that developed functional protective coatings for fabrics [54–58], no *ad hoc* protocol for simulating cotton ageing (relevant to long exposure to light and air) under oxidation conditions has been proposed and tested, with little attention paid to chemical changes over the cellulose fiber surfaces [54].

In this study, an antioxidant transparent fluorine-free hydrophobic treatment was designed for the conservation of cotton-based heritage textiles. Cotton fabric was functionalized with food-grade antioxidant butylated hydroxytoluene (BHT) embedded in polycaprolactone (PCL) as a first layer. A second layer of polydimethylsiloxane (PDMS) was applied over the antioxidant coating for water repellency [55]. In addition, an aggressive oxidation protocol was implemented, consisting of exposing the fabrics to H_2O_2 and UV–vis light to simulate an accelerated exposure to harsh oxidation medium. The antioxidant functionality of the coating was verified by radical scavenging activity tests and using infrared spectroscopy to monitor the chemical changes in the cotton surface. Developed double-layered coatings demonstrated excellent light transmission, water-repellency, antioxidant and mechanical properties achieved by using only ecofriendly and biodegradable polymers, making the treatment a valid candidate for the preservation of cultural heritage textiles.

The main goal of this work is to formulate a hydrophobic cotton treatment free from fluorinated chemicals or polymers but also with polymers or chemicals that are known to be biodegradable, biocompatible and nontoxic. Both PCL and PDMS satisfy these requirements along with food grade BHT. Furthermore, the lipophilic food-grade BHT crystals were easily dispersed within the hydrophobic PCL polymer by using a green co-solvent, benzyl alcohol. Subsequently, a PDMS coating improved the hydrophobicity of the fabric. Note that since the fabrics were dip coated in respective PCL and PDMS solutions with proper polymer concentrations (~2 wt.%), rather than forming a continuous film or coating over the fabrics, we mainly coated individual fiber surfaces with both polymers enabling pore breathability.

2. Materials and methods

2.1. Materials

Plain-woven and bleached 100 % cotton fabric, with 180 ± 5 g/m^2 mass density, was selected for the experiments. The textile has 24 threads/cm density both in warp and weft direction. Powdered polycaprolactone (hereafter, PCL) was supplied by Polysciences, Inc. (USA). The antioxidant butylated hydroxytoluene (hereafter BHT) and hydrogen peroxide (H_2O_2) solution 30 % (w/w) in water were purchased from Sigma-Aldrich. Single component acetoxy moisture cured polydimethylsiloxane resin (hereafter PDMS), a transparent silicone elastomer (ELASTOSIL®E43), was purchased from Wacker (Germany).

2.2. Preparation of the active coatings

The solution for the antioxidant coating was prepared by dissolving 0.50 g of powdered PCL in 25 mL of benzyl alcohol by stirring for 2 h at room temperature. When PCL was completely dissolved, 0.50 g of BHT

were added to the solution and the system was stirred for another 30 m. Afterwards, 25 mL of acetone were added in order to increase the volatility of the solution. In Fig. 1a, the preparation of the antioxidant coating is schematically represented. The solution for the hydrophobic coating was obtained by dissolving 1.00 g of PDMS in 50 mL of heptane, as represented in Fig. 1**b**. The components were stirred for 24 h, achieving a 2 % (w/v) homogeneous solution.

2.3. Application of the coatings

Prior to use, the cotton fabric was washed (standard detergents), rinsed and dried to remove any contamination. Samples of pure cotton fabric were labeled as COT. The cotton fabrics of 6 × 15 cm^2 were dipped in the antioxidant solution (PCL-BHT 2% w/v) for 30 s and allowed to dry at 40 °C for 24 h. The process was repeated two more times after the treated textiles dried. These samples were labeled as COT-AO, as reported in Table. 1. For the secondary hydrophobic coating, COT-AO fabrics were immersed in the PDMS (2% w/v in heptane) solution for 30 s and then dried at 40 °C for 24 h. For the second coating, the heating step was required not only to dry the sample but also to accelerate silicone crosslinking. The samples with the secondary protective PDMS layer were labeled as COT-AOP. Another control sample was produced by applying only PDMS layer to the cotton fabric, COT-P. Note that the drying temperature of 40 °C was chosen to ensure that if such a treatment was applied on a real historical/ancient fabric, complications due to thermal annealing would be minimized. Further experimental details on mechanical characterization, accelerated ageing and oxidation treatments, antioxidant properties characterization [59, 60], and color variation [61] are presented in the Supplementary Material as sections 2.9 to 2.12.

2.4. Morphological characterization by SEM

Scanning electron microscopy (SEM) was used to analyze the micromorphology of fiber surfaces and cross-sections of the samples. JEOL JSM- 6490LA (Japan), with 10 kV acceleration voltage, was used to acquire SEM images. Ten nm thick film of gold (Cressington 208 h sputter coater, UK) was used to sputter-coat the fabrics' surfaces prior to imaging. SEM images were collected at the following magnifications: ×50, ×1000, ×2000.

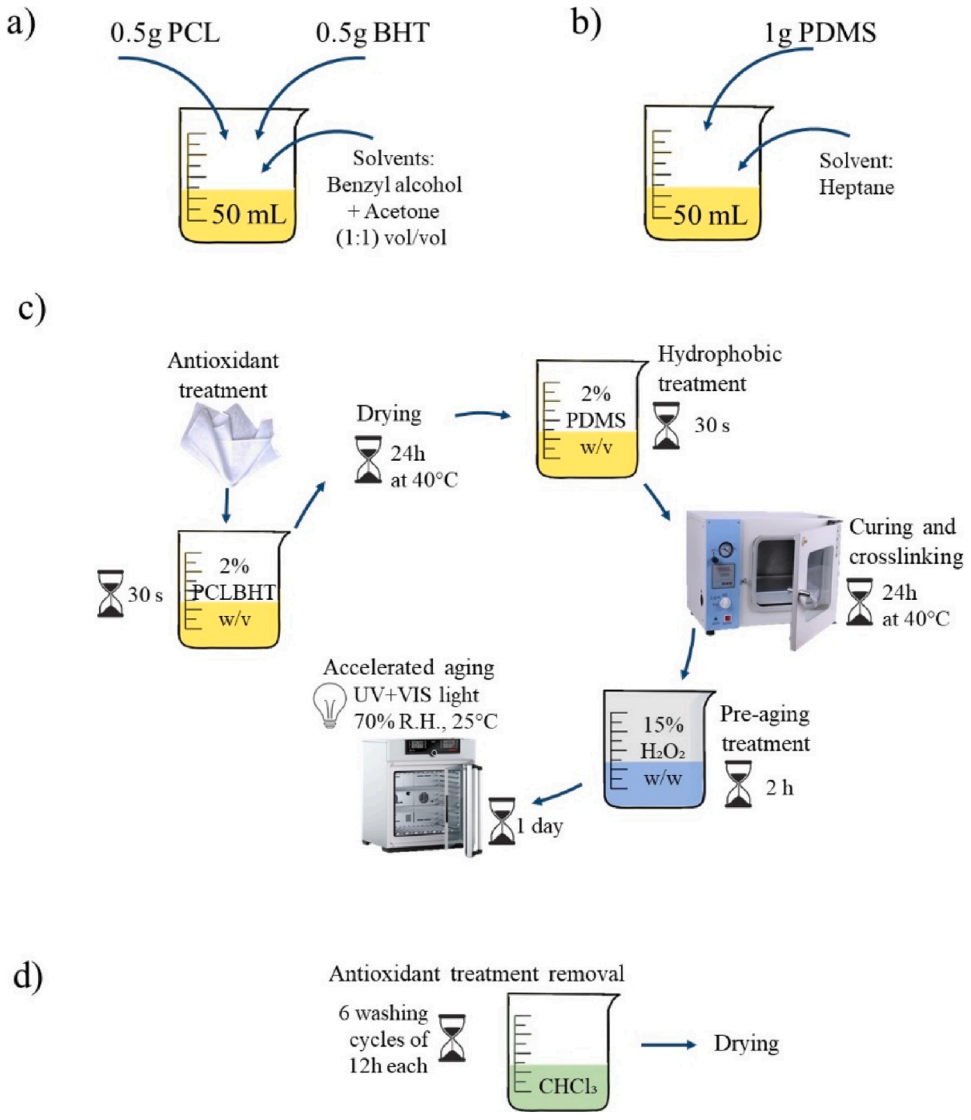

Fig. 1. Schematic representations of the preparation of (a) antioxidant and (b) hydrophobic coatings. A step-by-step representation of (c) coating, curing, and ageing processes for the fabric and (d) process for antioxidant polymeric layer removal. Fabric samples in the photos are about 5 × 5 cm in size.

2.5. Chemical characterization by attenuated total reflection–Fourier transform infrared (ATR-FTIR) spectroscopy

The instrument used to acquire infrared spectra is a single-reflection attenuated total reflection (ATR) accessory (MIRacle ATR, PIKE Technologies), with a diamond crystal coupled to a Fourier Transform Infrared (FTIR) spectrometer (VERTEX 70v, FT-IR, Bruker). The spectra were collected from 4000 to 600 cm^{-1} with a resolution of 4 cm^{-1}. Three spectra of 128 scans each were acquired for each sample.

2.6. Surface wettability by Water contact angle and water roll-off angle

Static water contact angles (WCA) were measured with a contact angle instrument (OCAH-200 DataPhysics, Germany) in order to investigate the fabrics' surface wettability. The analyses were performed at room temperature (~23 °C). Milli-Q water droplets of 5 μL were deposited through a gas-tight 500 mL Hamilton precision syringe with a blunt needle of 0.52 mm internal diameter [55,62]. Evolution of WCAs as a function of time was recorded by the software. Frames were taken from each video at 5 s, 10 s, and 60 s to compare the wettability of different surfaces. Reported WCA values were the average of ten droplets, which were deposited on each sample on different locations. Using the same instrument, the roll-off angle analysis was performed. Droplets of 15 μL, 20 μL, 25 μL, and 30 μL were deposited on the fabric surface, which was then tilted at an angular speed of 1.42° per second. Side view pictures of the drops were taken and the roll-off angle was recorded. For each sample, 5 measurements were performed.

2.7. Water vapor permeability

Water vapor permeability (WVP) of the uncoated and coated fabrics was determined at 25 °C and 100 % RH according to the ASTM E96 standard method. 100 % relative humidity was reached by placing 400 μL of deionized water in the sealed chambers of 7 mm × 10 mm inner volume. The samples were cut into circles with a diameter of 10 mm, they were placed on the chambers and then sealed. The chambers were moved in a desiccator where the outer environment was maintained at 0 % RH by silica gel desiccant. The transfer of water from the chamber, through the sample, to the desiccant was monitored by measuring the weight change of the chambers. The mass loss over time was registered by weighting samples every hour for 8 consecutive hours, with an electronic balance (with 0.0001 g accuracy). The mass loss of permeation chambers was plotted as a function of time. The slope of each line was calculated by linear regression. Then, the water vapor transmission rate (WVTR) was determined as below:

$$WVTR\left(g\left(m^2d\right)^{-1}\right) = \frac{slope}{area\ of\ the\ sample}$$

The water vapor permeability (WVP) of the samples was calculated with the following formula:

$$WVP\left(g(mdPa)^{-1}\right) = \frac{WVTR \cdot L \cdot 100}{p_s \cdot \Delta RH}$$

where L (m) is the thickness of the sample, measured with a micrometer with 0.001 mm accuracy, ΔRH (%) is the percentage relative humidity gradient, and p_s (Pa) is the saturation water vapor pressure at 25 °C. The tests were repeated three times for each sample.

2.8. Water uptake

Water uptake measurements on the untreated and treated fabric samples were also carried out. Samples were first placed in a dry chamber with anhydrous silica gel desiccant for 24 h. Dry samples were weighed on a sensitive electronic balance (0.0001 g accuracy) and placed in the humidity chamber at 100 % RH. After 24 h in the humidity chamber, each sample was weighed every day and the amount of adsorbed water was calculated based on the initial dry weight as the difference, according to the following formula:

$$Water\ adsorption\ (\%) = \frac{m_f - m_0}{m_0} \cdot 100$$

Where m_f is the sample weight at 100 % RH condition and m_0 is the sample at 0 % RH. The test proceeded until stabilization of the weight gain. The trend of mass increase over time is reported.

3. Results and discussion

3.1. Morphological characterization

The morphology of the COT, COT-AO, COT-AOP and COT-P samples was analyzed by using SEM microscopy. Figure **2a** shows the dense woven structure of the untreated fabric (COT). The typical wrinkle-like and longitudinal fibril structure [63,64] of cotton fibers can be observed at ×2000 magnification (Fig. 2**a**). The cross-section of the warp at ×1000 magnification highlighted the sharp section of each fiber without any fall-out or partial filament separation among them. On the other hand, in the COT-AO samples, some polymeric traces are visible at ×2000 in Fig. 2**b**. A similar finding was noticed in the cross-sectional image, where some polymeric filaments due to the coating were visible among the fibers at ×1000 magnification (highlighted by the yellow arrow). However, the morphological aspect of COT-AO at low magnification (×50) appears comparable to the untreated one, suggesting that the antioxidant treatment did not alter the macroscopic appearance of the fabric and conformed to the fiber surfaces.

Finally, the morphology of COT-P and COT-AOP samples is reported in **c** and Fig. 2**d**. Similar to the COT and COT-AO, the woven structures of the COT-P and COT-AOP samples remained unchanged. However, the presence of pure PDMS or the double polymeric coating (PCL + PDMS) was confirmed by the formation of a smoother fiber surface compared to the untreated fabric in Fig. 2**a**. Moreover, in the cross-sectional SEM images at ×1000, polymeric filaments among the fibers can be noticed.

Even though, the treatments were invisible to the naked eye, they changed the weight and the thickness of the fabrics. In Table 1 the detailed data are reported. Due to the antioxidant treatment, the fabric thickness and the mass density (*i.e.*, grams per meter square GSM) increased by 4.7 % and 5.3 %, respectively. Similarly, after applying both the antioxidant and the hydrophobic layers, the fabric thickness and the mass density increased by 5.0 % and 7.9 % respectively.

3.2. Chemical characterization

3.2.1. Infrared spectroscopy characteristics of the coatings

Typical bands of cotton [65,66] are shown in Fig. 3**a**: stretching of O—H groups at 3329 and 3283 cm^{-1}, asymmetrical and symmetrical stretching of CH_2 at 2897 cm^{-1} and 2866 cm^{-1}, OH— bending of the adsorbed water at 1643 cm^{-1}, CH_2 scissoring at 1427 cm^{-1}, C–H bending at 1364 cm^{-1}, CH_2 rocking at 1314 cm^{-1}, CO— stretching at 1201 cm^{-1}, asymmetrical bridge C—OC— stretching at 1159 cm^{-1}, asymmetric in-plane C—OC— stretching band at 1105 cm^{-1}, asymmetric and symmetric C—O stretch at 1053 and 1028 cm^{-1}, respectively, ring stretching modes at 986 cm^{-1} and ß-Linkage of cellulose at 897 cm^{-1}. No CO═ stretching in the spectral region 1800−1700 cm^{-1} is detected in the COT samples.

The antioxidant coating was composed of the antioxidant molecule BHT and the biodegradable polymer PCL and their FTIR spectra are reported in Fig. 3**a**. The main bands of BHT that are associated with the chemical structure of the antioxidant molecule are [67]: sharp stretching of O—H at 3624 cm^{-1}, weak aromatic C–H stretching at 3071 cm^{-1}, asymmetrical and symmetrical stretching of CH_2 at 2953 cm^{-1} and 2911 cm^{-1}, CC═ aromatic stretching at 1431 cm^{-1}, CO— stretching at 1148

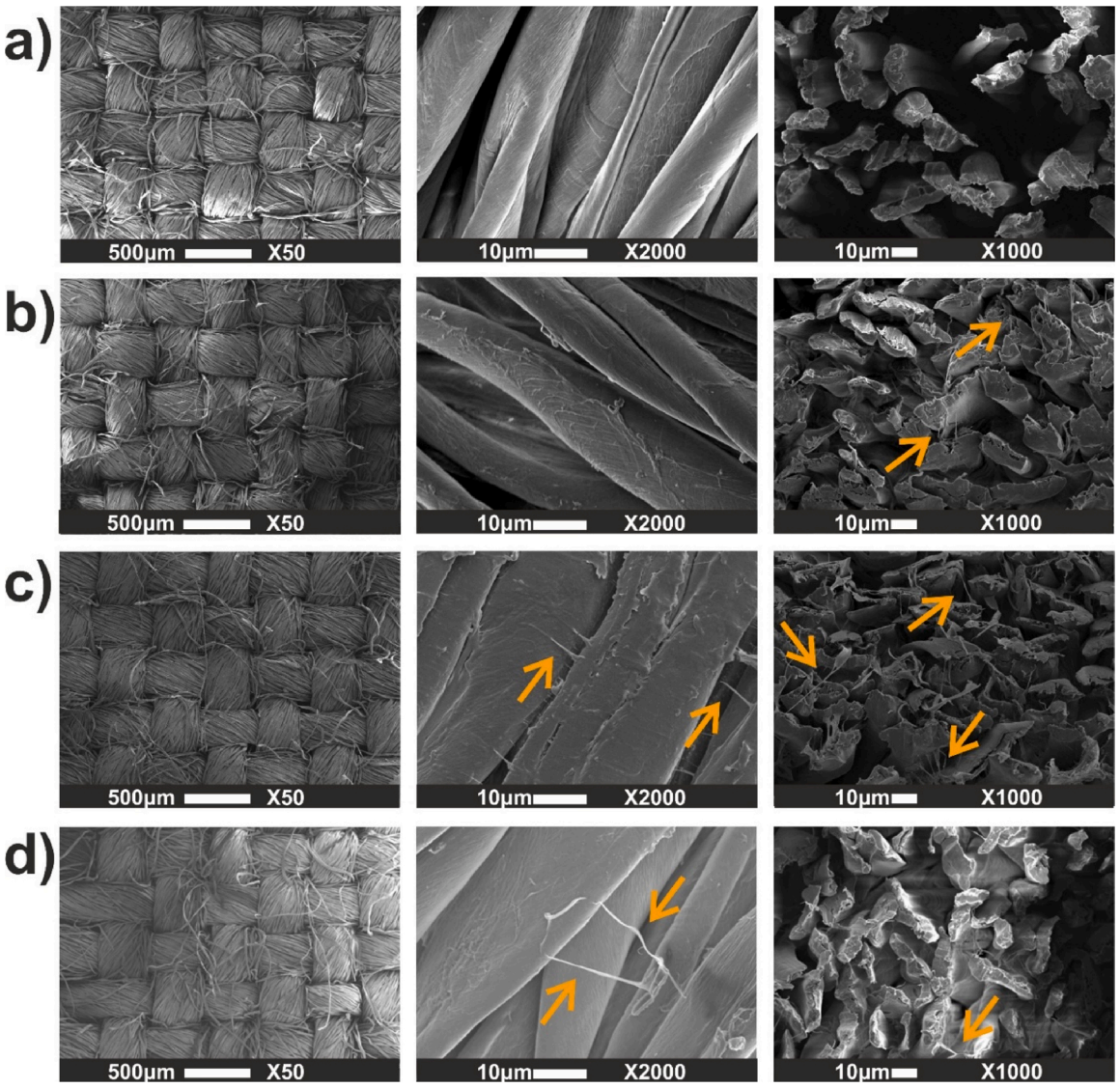

Fig. 2. SEM images of (a) COT: untreated sample, (b) COT-AO: cotton with the antioxidant treatment of PCL and BHT, (c) COT-AOP: cotton with the antioxidant treatment of PCL and BHT and hydrophobic treatment of PDMS. (d) COT-P: cotton treated only with PDMS. In each row, there are SEM images of the top-view at ×50 (on the left) and ×2000 (middle) magnifications, and their corresponding cross-sectional images at ×1000 magnification (on the right). The arrows indicate the presence of polymeric materials.

Table 1
Names, thickness and weight/area of samples.

Sample names	Thickness (µm)	Percent increase in thickness (Δµm%)	GSM (Grams per Square meter)	Percent increase in GSM (Δg/m^2%)
COT	297 ± 2	–	189 ± 1	–
COT-AO	311 ± 2	4.7 %	199 ± 2	5.3 %
COT-P	312 ± 1	4.7 %	202 ± 3	7.7%
COT-AOP	312 ± 3	5.0 %	204 ± 2	7.9 %

cm^{-1}. In the PCL spectrum, bands were ascribed to characteristic absorptions of the polymer [68]: asymmetric and symmetric stretching of CH_2 at 2942 and 2866 cm^{-1}, the sharp peak of C═O stretching at 1724 cm^{-1}, asymmetric and symmetric stretching of C—OC at 1238 cm—$^{-1}$ and 1162 cm^{-1} respectively. After the coating process, the spectrum of COT-AO samples is mainly characterized by the peaks of the cotton, although the C═O stretching peak typical of PCL appeared at 1724 cm^{-1}, confirming the coating presence.

A PDMS coating was also made directly on the cotton textile as a control for the hydrophobic coating. PDMS spectrum is reported in Fig. 3**a** and shows typical bands of the silicone material: asymmetric and symmetric CH_3 stretching at 2963 and 2905 cm^{-1}, respectively, symmetric CH_3 bending mode at 1258 cm^{-1}, symmetric and asymmetric Si–O–Si stretching modes at 1063 and 1005 cm^{-1}, respectively, CH_3 rocking mode at 795 cm^{-1} [69]. In the FTIR spectrum of the COT-P sample, the presence of the hydrophobic coating was confirmed by the increase in intensity of the peak at 1258 cm^{-1} and by the appearance of CH_3 rocking mode at 795 cm^{-1}, characteristic of PDMS, among all the typical peaks of cellulose. These outcomes confirmed that when the hydrophobic coating is applied on the fabric, a thin layer of PDMS was deposited on the surface of every fiber, as it was also noticed in the morphological analyses. It has to be noted that PDMS does not show any peak in the carbonyl area; thus, no bands were found in the area of 1750−1720 cm^{-1} in the sample COT-P.

3.2.2. *Infrared spectroscopy results after accelerated ageing and oxidation*

In the natural ageing process of the cellulose, it is well known that oxidative processes occur and carbonyl groups appear in the polysaccharide backbones, as found in 400 and 500 year-old cellulose

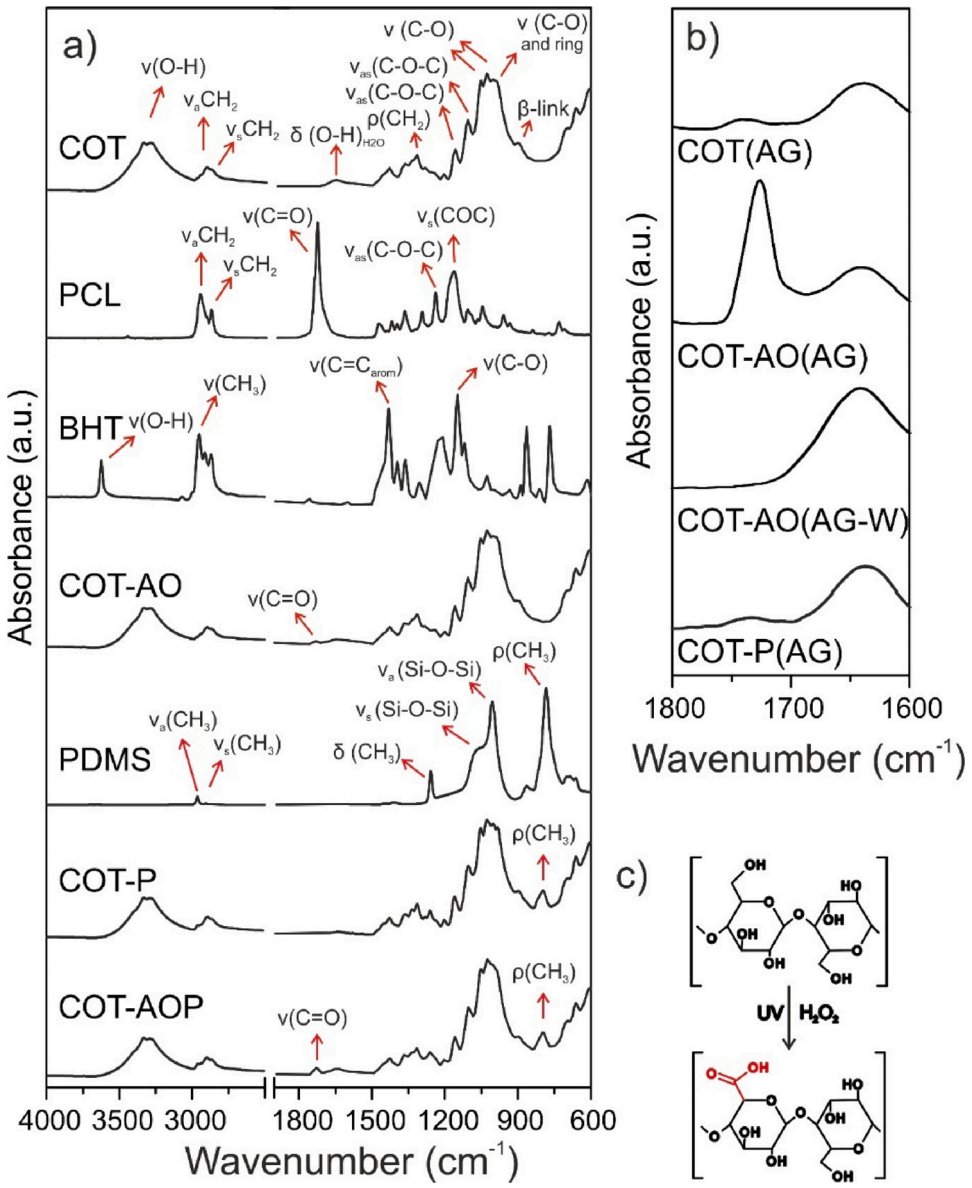

Fig. 3. (a) ATR-FTIR spectra of cotton fabric, PCL, BHT, COT-AO, PDMS, COT-P, and COT-AOP in the 4000 - 600 cm^{-1} region. The main assignments for cotton, BHT, PCL and PDMS are included. (b) the region at 1800 – 1600 cm^{-1} where the carbonyl band appears in the samples COT(AG), COT-AO(AG), and COT-P(AG), while it is not visible in the sample COT-AO(AG—W). (c) A representative model of the chemical reaction occurring in cellulose through the accelerated ageing treatment.

samples reported by Boukir et al. [70]. Furthermore, cellulose paper dated CE 1955 and 1973 described by Librando et al. [71] and textile cotton fibers dated A.D. 1250–1300, 900–1100, 1325–1400 analyzed by Cardamone et al. [72] presented the characteristic peak in the spectral region 1750−1720 cm^{-1}, associated with the C═O stretching of the oxidation.

Before ageing, the C═O peak, correlated with the oxidation of the cellulose at ca. 1740 cm^{-1} is not present in the sample COT (pristine cotton fabric) (Fig. 3a**)**. After the ageing, in the spectrum of the sample COT(AG) an oxidation peak appeared at 1740 cm^{-1}, as shown in Fig. 3b, confirming oxidation process [73]. Hence, the new peak can be associated with an oxidative reaction on C_6 of the cellulose structure, where the CH_2OH group is oxidized to COOH. A schematic of the oxidation reaction is shown in Fig. 3**c**.

To verify the efficiency of the antioxidant coating, the samples COT-AO were subjected to the ageing process treatment. As the COT-AO(AG) had the peak of C═O group associated with the PCL (1724 cm^{-1}) in the same area of the oxidation marker of cellulose, COT-AO(AG) samples after ageing were soaked in chloroform in order to remove the PCL. The spectrum of sample COT-AO(AG) after PCL removal, named COT-AO (AG—W), is reported in Fig. 3**b**. After chloroform etching of the PCL, in the spectral region 1750−1720 cm^{-1}, no peaks could be attributed neither to PCL nor to oxidation related peaks, confirming the removal of the polymer and excellent efficacy of the antioxidant coating. To ensure that washing with chloroform does not remove or alter oxidation peak associated with aged-cellulose, pure cotton fabrics underwent the same ageing process (COT-AG) and were washed or soaked in chloroform six consecutive times; at the end of this treatment the oxidation peak was still present (not shown for brevity).

As for the sample COT-P(AG), upon accelerated ageing, the peak at 1740 cm^{-1} is noticeable, meaning that the cellulose was oxidized even when the PDMS hydrophobic coating was applied. As described in literature [74,75], PDMS is known to have poor gas and moisture barrier properties. Despite the good hydrophobicity of PDMS, it appears to be inefficient in preventing accelerated oxidation of the underlying cellulose, confirming the need to apply a functional coating before the hydrophobic treatment.

3.3. Treated textile hydrophobicity, water vapor permeation and water uptake measurements

The wettability of the cotton fabrics was studied by measuring static water contact angle. The water contact angle on the sample COT was not possible to be measured, as the deposited water droplet was immediately absorbed into the fabric. In general, cotton fibers are prone to absorb a significant amount of water due to their high hygroscopicity [3,17]. However, it was possible to report the WCA on the sample COT-AO, since the droplet took approximately 10 s to be absorbed by the substrate, as reported in Fig. 4**a**. A highly hydrophobic surface was obtained by the PDMS coating. Indeed, the sample COT-AOP maintained a WCA of ~144°, and the water never sank in the substrate throughout the observation period (evaporated away after sufficient time), see Fig. 4**a**.

In addition, roll-off angles of water droplets with varying droplet volume were measured to quantify dynamic surface wettability. The tests were not performed on COT and COT-AO, since the surfaces absorbed water droplets, as shown in Fig. 4**a**. Fabrics having the PDMS layer *i.e.,* the samples COT-P and COT-AOP showed water roll-off angles of 35° and 52°, respectively, when water droplets with a volume of 15 μL or larger were used. Droplet mobility with lower roll-off angles for larger volume droplets was found for both treatments. This can be ascribed to competition between gravitational and surface tension forces, as shown in Fig. 4**b** [76]. Between the two samples, the COT-P has better self-cleaning properties as compared to the COT-AOP, because of the presence of PCL underneath the PDMS. Nevertheless, the treated sample COT-AOP could hold large droplets volumes (~100 μL of colored water) on its surface without spreading, as shown in Fig. 4**b.**

The breathability of the treated cotton fabrics was measured through water vapor permeability (WVP) test. PCL-BHT and PDMS treatments are respectively intended to confer antioxidant and hydrophobic properties to the fibers. However, they should avoid occluding the pores of the fabrics to prevent the accumulation of humidity with all its consequences. The average WVTR of the untreated cotton is calculated to be ~ 5866 ($g/m^2 \cdot day$), which corresponds to WVP ~ $5.5 \cdot 10^{-4}$ g (m day Pa)$^{-1}$. Indeed woven cotton is demonstrated to be highly breathable. After the antioxidant and hydrophobic treatments, all analyzed samples showed WVP values comparable to the original fabric and decreased only by 8% for COT-AO and 9% for COT-AOP, as shown in Fig. 4**d**. Comparable breathability to the pristine cotton fabric could be obtainable thanks to the maintained porosity of the textile, as it was confirmed through the SEM images in Fig. 2, where it is visible that the porosity between the warp and weft threads is maintained after the applied treatments.

Water vapor uptake was monitored in 100 % RH for 5 consecutive days, till the mass change reached equilibrium. After 5 days, there was no significant variation and at this point, the maximum quantity of the water vapor was absorbed. Fig. 4**c** shows that the water vapor uptake of the sample COT arrived to 8.3 ± 0.2 % with respect to the starting weight. As expected, PDMS did not play a significant role in the protection from water vapor. In fact, PDMS is known to be permeable to water vapor [74,75] and the water vapor uptake of the sample COT-P is 7.6 ± 0.2 %, i.e. slightly lower than COT. In contrast, the antioxidant layer played a major role in the prevention of water uptake. The samples COT-AO and COT-AOP displayed a mass change of 6.1 ± 0.1 % and 6.2 ± 0.1 %, respectively, compared to the initial mass (see Fig. 4c). Hence, the protective layers did not affect the breathability and the porosity of the fabrics, keeping the natural properties of cotton unchanged, while they were efficient in the reduction of water uptake capacity of the fabrics. This outcome is essential to reduce swelling, shrinking, biological attack and biodeterioration, due to the presence of adsorbed water on the fabric.

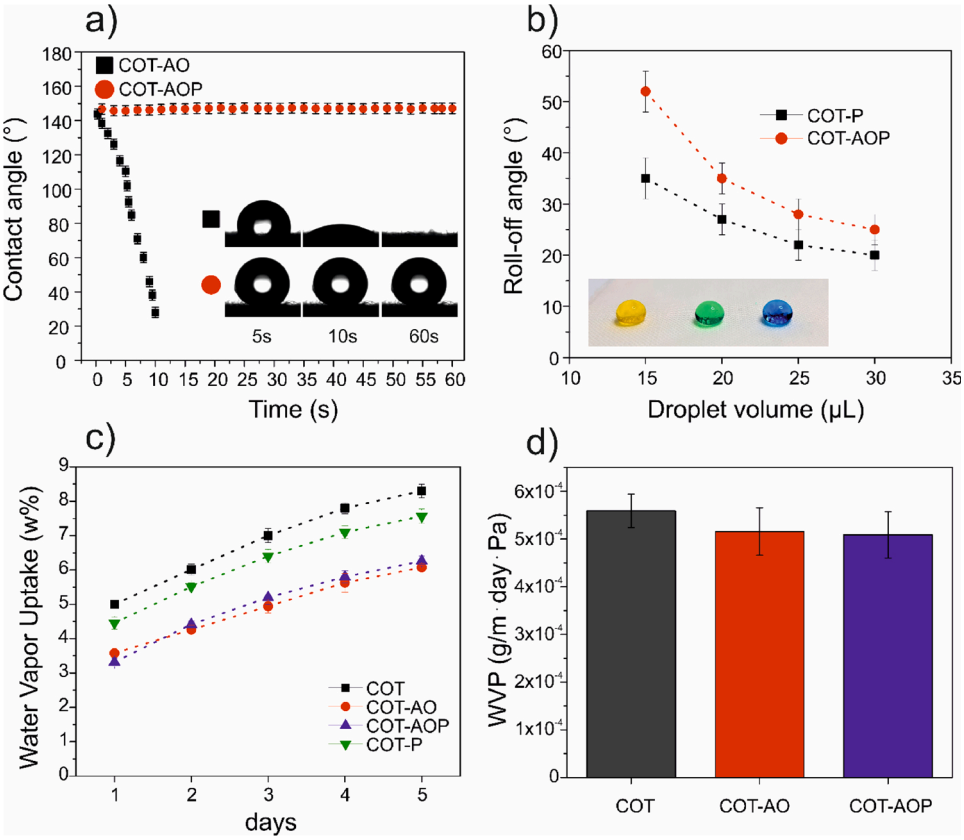

Fig. 4. (a) Water contact angles as a function of droplet deposition time. Static WCA are reported at 5 s, 10 s, 60 s for the samples COT-AO and COT-AOP. (b) Water roll off angle of the samples COT-AOP and COT-P0; colored water droplets of 100 μL onto the sample COT-AOP. (c) Water vapor uptake of the samples COT, COT-AO, COT-AOP and COT-P kept at 100 % R.H. for 5 days. (d) Water vapor permeability of the samples COT, COT-AO and COT-AOP.

3.4. Mechanical characterization

In Fig. 5**a** the standard tensile stress-strain curves of the samples COT, COT-AO and COT-AOP samples are reported. The first part of the slope (from 0 to 0.1 mm/mm) in the stress-strain curves coincides with the strain in the single yarn, which increases under moderate stress, lengthens and tries to resist further stress-induced deformations. The second part of the slope (from 0.1 mm/mm on) represents to the irreversible stretching after overcoming the initial strain levels, and individual fibers start elongating within the woven network [55]. The Young's modulus associated with both slopes is reported in Fig. 5**b**. In particular, the elastic modulus was measured to be ~270 ± 25 MPa for the sample COT, ~287 ± 12 MPa for the sample COT-AO and ~228 ± 8 MPa for the sample COT-AOP. In Fig. 5**c** the values of stress at maximum load for each sample are shown. A decreasing trend of the ultimate tensile stress from ~50 ± 3 MPa for the sample COT (pristine cotton fabric) to ~39 ± 3 MPa and ~42 ± 2 MPa for the samples COT-AO and COT-AOP, respectively, was found.

Finally, Fig. 5**d** shows the results of maximum elongation at break. The pristine cotton fabric (sample COT) displayed a maximum elongation at break point of ~37 ± 2 %. While the treated samples COT-AO and COT-AOP reached an elongation of ~26 ± 2 % and ~31 ± 2 %, respectively. Overall, the treatment did not cause a remarkable variation in the mechanical properties of the starting woven cotton fabric.

3.5. Radical scavenging activity

$^{\bullet}ABTS^{+}$ radical assay was used to determine the free radical scavenging activity of the antioxidant coating applied onto the cotton fabrics. The radical inhibition effect is manifested through a discoloration, from an intensely blue of the cation radical $ABTS^{\bullet+}$ to colorless solution. Fig. 6**b** represents the color loss of the $ABTS^{\bullet+}$ radical solution after immersing the COT-AO and COT-AOP samples into it for 24 h and demonstrates an effective antioxidant response.

In Fig. 6a, the radical scavenging activity (RSA) of the samples COT-AO and COT-AOP against the radical cation $ABTS^{\bullet+}$ solution is represented. The samples COT-AO and COT-AOP reached 82 ± 1 % and 87 ± 1% inhibition level, respectively, after 24 h of immersion in the radical aqueous solution. Considering that PCL and PDMS do not show any antioxidant property [77,78] the obtained antioxidant activity can be attributed to the presence of BHT in the cotton matrix, conferring a suitable scavenging action. Note that our main goal was to immobilize or coat the cotton fibers with 100 % BHT only. However, it crystalizes rapidly out of solution and does not form continuous films. Hence, we combined it with PCL in equal weights in solution (see Section 2.2). As such, it is not an additive but a main coating component bonded to cotton fibers with the help of PCL resin. In general, phenolic antioxidants are added to polymers between 0.01 % to 0.1 % [56–60]. In the present work, BHT concentration is at least two orders of magnitude higher. Radical scavenging activities of the fabrics COT-AO and COT-AOP were also measured after accelerated ageing tests (COT-AO (AG); COT-AOP(AG)) and no differences were observed with the data reported in Fig. 6**a** (see **Figure S1** in the Supplementary Material).

3.6. Color variation

Fig. 6**c** shows the measured colorimetric variations of the samples COT-AO, and COT-AOP, as well as the respective ones after accelerated natural ageing process COT-AO(AG) and COT-AOP(AG), with respect to the sample COT. All color variations (ΔE) are much lower than 3, *i.e.,* 0.35 ± 0.05 for the sample COT-AO, 1.75 ± 0.06 for COT-AO(AG), 0.53 ± 0.08 for COT-AOP, and 1.98 ± 0.07 for COT-AOP(AG). **Figure S2** (Supplementary Material) also shows photographs of the treated fabrics with no color variation compared to the untreated one. Therefore, the proposed treatments are appropriate and beneficial for Heritage-related fabrics application [61].

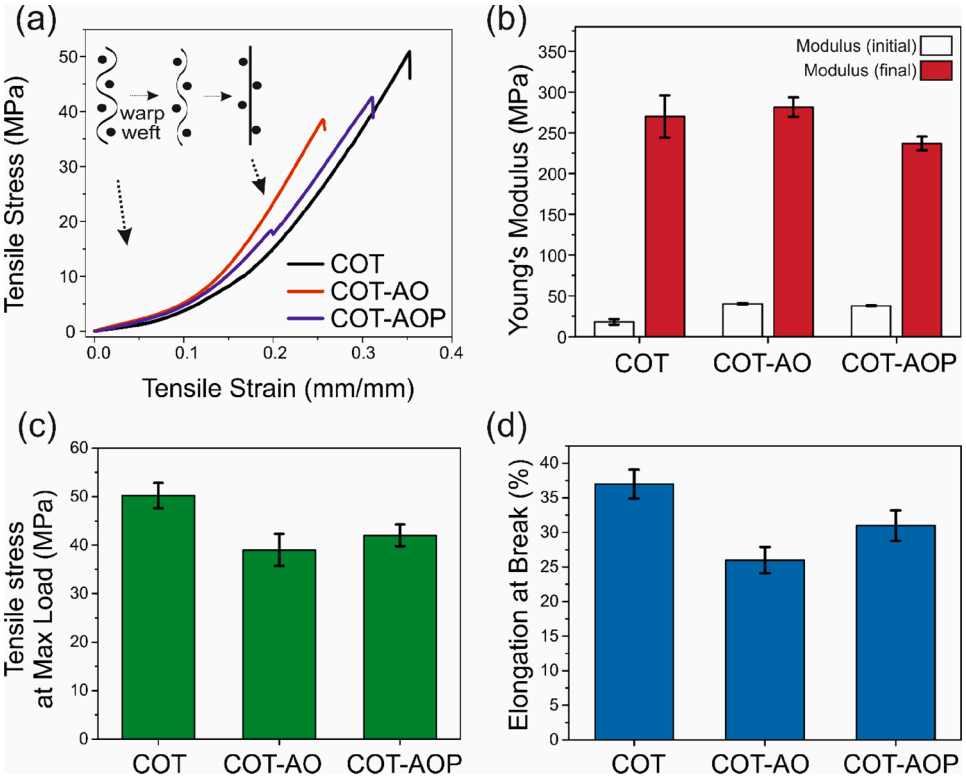

Fig. 5. Mechanical tests performed on the samples COT, COT-AO and COT-AOP. (a) stress strain curves, (b) Young's modulus calculated on the first (0 to 0.1 mm/mm) and the second (0.1 mm/mm on) slopes, (c) tensile stress at maximum load, and (d) maximum elongation at breakpoint.

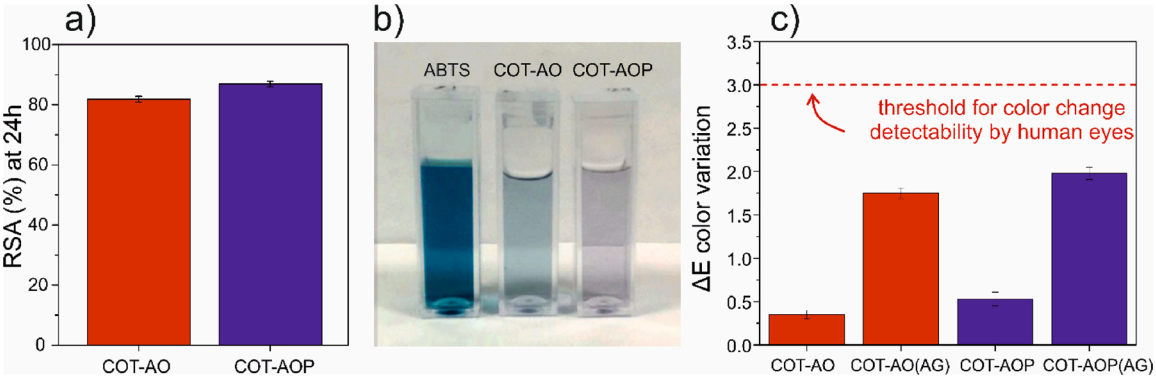

Fig. 6. (a) Radical scavenging activity. (b) Cuvettes containing the $ABTS^{\bullet+}$ radical solution without sample, the samples COT-AO and COT-AOP in the $ABTS^{\bullet+}$ radical solution after 24 h. (c) ΔE color variation.

4. Conclusions

Woven cotton fabrics were treated with a double layer polymer coating comprising a biodegradable polymer (PCL) and a biocompatible hydrophobic polymer (PDMS) for protection against oxidative ageing and degradation, while rendering them hydrophobic. A food-grade common antioxidant known as BHT was incorporated into the PCL layer that remained effective against aggressive accelerated peroxide and UV ageing conditions, simulating decades of atmospheric ageing. The PDMS-based outer coating was hydrophobic and prevented wetting of the fabrics. The dual-functional coating maintained the textile morphology with minimal impact on mechanical properties and breathability. This work shows that textiles based on cellulose can be protected against oxidative ageing by a simple treatment using eco-friendly resins and processes. Moreover, an *ad hoc* protocol for simulating in only 24 h the long-term cotton ageing under oxidative conditions had been proposed and tested. The developed protocol has been used to prove the efficiency of the presented protective treatment.

CRediT authorship contribution statement

Giulia Mazzon: Conceptualization, Methodology, Writing - original draft. **Marco Contardi:** Methodology, Data curation. **Ana Quilez-Molina:** Methodology, Data curation. **Muhammad Zahid:** Methodology, Data curation. **Elisabetta Zendri:** Supervision, Writing - review & editing. **Athanassia Athanassiou:** Supervision, Writing - review & editing. **Ilker S. Bayer:** Supervision, Conceptualization, Methodology, Investigation, Writing - review & editing.

Declaration of Competing Interest

The authors declare that they have no known competing financial interests or personal relationships that could have appeared to influence the work reported in this paper.

Appendix A. Supplementary data

Supplementary material related to this article can be found, in the online version, at doi:https://doi.org/10.1016/j.colsurfa.2020.126061.

References

[1] A. Geijer, A History of Textile Art, Pasold Research Fund in Association With Sotheby Parke Bernet, Biblio Distribution Center, London: Totowa, N.J, 1979.
[2] P.H.M. Association (HMA), ICCROM, Conserving Textiles: Studies in Honour of Ágnes Timár-balázsy, 2009.
[3] G. Mazzon, I. Zanocco, M. Zahid, I. Bayer, A. Athanassiou, L. Falchi, E. Balliana, E. Zendri, Nanostructured coatings for the protection of textiles and paper, Ge-Conservación/Conservação. (2017) 180–188.
[4] O. Abdel-Kareem, Investigation and conservation of a historical woman's coat decorated with Fur parts, JTATM. 7 (2011) 12.
[5] L. Bílková, Application of infrared spectroscopy and thermal analysis to the examination of the degradation of cotton fibers, Polym. Degrad. Stab. 97 (2012) 35–39, https://doi.org/10.1016/j.polymdegradstab.2011.10.018.
[6] C. Margariti, The application of FTIR microspectroscopy in a non-invasive and non-destructive way to the study and conservation of mineralised excavated textiles, Herit. Sci. 7 (2019), https://doi.org/10.1186/s40494-019-0304-8.
[7] L. Fuster-López, F.C. Izzo, M. Piovesan, D.J. Yusá-Marco, L. Sperni, E. Zendri, Study of the chemical composition and the mechanical behaviour of 20th century commercial artists' oil paints containing manganese-based pigments, Microchem. J. 124 (2016) 962–973, https://doi.org/10.1016/j.microc.2015.08.023.
[8] C.M. Grzywacz, Monitoring for Gaseous Pollutants in Museum Environments, Getty Conservation Institute, Los Angeles, Calif, 2006.
[9] M.M.Á.D. Maciel, K.C.C. de C. Benini, H.J.C. Voorwald, M.O.H. Cioffi, Obtainment and characterization of nanocellulose from an unwoven industrial textile cotton waste: effect of acid hydrolysis conditions, Int. J. Biol. Macromol. 126 (2019) 496–506, https://doi.org/10.1016/j.ijbiomac.2018.12.202.
[10] Y.W. Chen, H.V. Lee, J.C. Juan, S.-M. Phang, Production of new cellulose nanomaterial from red algae marine biomass Gelidium elegans, Carbohydr. Polym. 151 (2016) 1210–1219, https://doi.org/10.1016/j.carbpol.2016.06.083.
[11] G. Liu, P. Han, L. Chai, Z. Li, L. Zhou, Fabrication of cotton fabrics with both bright structural colors and strong hydrophobicity, Colloids Surf. A Physicochem. Eng. Asp. (2020), 124991.
[12] B. Gutarowska, K. Pietrzak, W. Machnowski, J.M. Milczarek, Historical textiles – a review of microbial deterioration analysis and disinfection methods, Text. Res. J. 87 (2017) 2388–2406, https://doi.org/10.1177/0040517516669076.
[13] L.E. Castrillón Rivera, J.I. Castañeda Sánchez, M. Elisa Drago Serrano, A.P. Ramos, Origin and control strategies of biofilms in the cultural heritage, in: antimicrobials, antibiotic resistance, antibiofilm strategies and activity methods, IntechOpen (2019), https://doi.org/10.5772/intechopen.79617.
[14] M. Silva, T. Rosado, M. Gonzalez-Pérez, D. Gobbo, D. Teixeira, A. Candeias, A. T. Caldeira, Production of Antagonistic compounds by Bacillus sp. with Antifungal activity against Heritage Contaminating Fungi, Coatings. 8 (2018) 123, https://doi.org/10.3390/coatings8040123.
[15] F. Palla, G. Barresi (Eds.), Biotechnology and Conservation of Cultural Heritage, Springer International Publishing, Cham, 2017, https://doi.org/10.1007/978-3-319-46168-7.
[16] M. Gacto, M. Gacto, Los microorganismos y el arte, An. Biol. 33 (2011) 107–115.
[17] A. Timar-Balazsy, D. Eastop, Chemical Principles of Textile Conservation, Routledge, London, 1998.
[18] L. Falchi, E. Zendri, U. Müller, P. Fontana, The influence of water-repellent admixtures on the behaviour and the effectiveness of Portland limestone cement mortars, Cem. Concr. Compos. 59 (2015) 107–118, https://doi.org/10.1016/j.cemconcomp.2015.02.004.
[19] K. Asche, P. Cox Crews, An evaluation of antioxidants for the conservation of museum textiles, Cloth. Text. Res. J. 6 (1988) 10–16, https://doi.org/10.1177/0887302X8800600302.
[20] S.J. Hackney, G.A. Hedley, The deterioration of linen canvas: accelerated aging tests to investigate the modes of deterioration and to assess retarding treatments, Stud. Conserv. 27 (1982) 151–153, https://doi.org/10.1179/sic.1982.27.Supplement-1.151.
[21] P.A. Annis, Understanding and Improving the Durability of Textiles, Elsevier, 2012.
[22] A. Quye, Factors influencing the stability of man-made fibers: a retrospective view for historical textiles, Polym. Degrad. Stab. 107 (2014) 210–218, https://doi.org/10.1016/j.polymdegradstab.2014.03.002.
[23] O.M.A. Abdel-Kareem, The long-term effect of selected conservation materials used in the treatment of museum artefacts on some properties of textiles, Polym. Degrad. Stab. 87 (2005) 121–130, https://doi.org/10.1016/j.polymdegradstab.2004.07.014.
[24] R.M. Rossi, R. Gross, H. May, Water vapor transfer and condensation effects in multilayer textile combinations, Text. Res. J. 74 (2004) 1–6, https://doi.org/10.1177/004051750407400101.

[25] I.S. Bayer, Superhydrophobic coatings from ecofriendly materials and processes: a review, Adv. Mater. Interfaces 7 (2020), 2000095, https://doi.org/10.1002/admi.202000095.
[26] X. Zhao, M. Sun, Y. Duan, H. Hao, Superhydrophobic coatings based on raspberry-like nanoparticles and their applications on cotton, Colloids Surf. A Physicochem. Eng. Asp. (2020), 125039.
[27] A. Colombo, F. Gherardi, S. Goidanich, J.K. Delaney, E.R. de la Rie, M.C. Ubaldi, L. Toniolo, R. Simonutti, Highly transparent poly(2-ethyl-2-oxazoline)-TiO2 nanocomposite coatings for the conservation of matte painted artworks, RSC Adv. 5 (2015) 84879–84888, https://doi.org/10.1039/C5RA10895K.
[28] M. Yang, W. Liu, C. Jiang, Y. Xie, H. Shi, F. Zhang, Z. Wang, Facile construction of robust superhydrophobic cotton textiles for effective UV protection, self-cleaning and oil-water separation, Colloids Surf. A Physicochem. Eng. Asp. 570 (2019) 172–181.
[29] Q. Xu, L. Shen, P. Duan, L. Zhang, F. Fu, X. Liu, Superhydrophobic cotton fabric with excellent healability fabricated by the “grafting to” method using a diblock copolymer mist, Chem. Eng. J. 379 (2020), 122401.
[30] J. Wu, J. Li, Z. Wang, M. Yu, H. Jiang, L. Li, B. Zhang, Designing breathable superhydrophobic cotton fabrics, RSC Adv. 5 (2015) 27752–27758, https://doi.org/10.1039/C5RA01028D.
[31] K. Sasaki, M. Tenjimbayashi, K. Manabe, S. Shiratori, Asymmetric Superhydrophobic/Superhydrophilic cotton fabrics designed by spraying polymer and nanoparticles, ACS Appl. Mater. Interfaces 8 (2016) 651–659, https://doi.org/10.1021/acsami.5b09782.
[32] C. Cao, M. Ge, J. Huang, S. Li, S. Deng, S. Zhang, Z. Chen, K. Zhang, S. Al-Deyab, Y. Lai, Robust fluorine-free superhydrophobic PDMS–ormosil@fabrics for highly effective self-cleaning and efficient oil–water separation, J. Mater. Chem. A 4 (2016) 12179–12187, https://doi.org/10.1039/C6TA04420D.
[33] J. Ou, F. Wang, W. Li, M. Yan, A. Amirfazli, Methyltrimethoxysilane as a multipurpose chemical for durable superhydrophobic cotton fabric, Prog. Org. Coat. 146 (2020), 105700, https://doi.org/10.1016/j.porgcoat.2020.105700.
[34] A.K. Singh, J.K. Singh, Fabrication of durable superhydrophobic coatings on cotton fabrics with photocatalytic activity by fluorine-free chemical modification for dual-functional water purification, New J. Chem. 41 (2017) 4618–4628, https://doi.org/10.1039/C7NJ01042G.
[35] Q. Liu, J. Huang, J. Zhang, Y. Hong, Y. Wan, Q. Wang, M. Gong, Z. Wu, C.F. Guo, Thermal, Waterproof, Breathable, and Antibacterial Cloth with a Nanoporous Structure, ACS Appl. Mater. Interfaces 10 (2018) 2026–2032, https://doi.org/10.1021/acsami.7b16422.
[36] N.F. Attia, M. Moussa, A.M.F. Sheta, R. Taha, H. Gamal, Effect of different nanoparticles based coating on the performance of textile properties, Prog. Org. Coat. 104 (2017) 72–80, https://doi.org/10.1016/j.porgcoat.2016.12.007.
[37] T. Zhu, S. Li, J. Huang, M. Mihailiasa, Y. Lai, Rational design of multi-layered superhydrophobic coating on cotton fabrics for UV shielding, self-cleaning and oil-water separation, Mater. Des. 134 (2017) 342–351, https://doi.org/10.1016/j.matdes.2017.08.071.
[38] W. Zhao, X. Xiao, G. Pan, Z. Ye, Fabrication of Cu species functionalized cotton fabric with oil/water separating reusability by in-situ reduction process, Surf. Coat. Technol. 385 (2020), 125405, https://doi.org/10.1016/j.surfcoat.2020.125405.
[39] D. Aslanidou, I. Karapanagiotis, C. Panayiotou, Superhydrophobic, superoleophobic coatings for the protection of silk textiles, Prog. Org. Coat. 97 (2016) 44–52, https://doi.org/10.1016/j.porgcoat.2016.03.013.
[40] M. Zahid, G. Mazzon, A. Athanassiou, I.S. Bayer, Environmentally benign non-wettable textile treatments: a review of recent state-of-the-art, Adv. Colloid Interface Sci. (2019), https://doi.org/10.1016/j.cis.2019.06.001.
[41] Q. Xu, L. Wang, F. Fu, X. Liu, Fabrication of fluorine-free superhydrophobic cotton fabric using fumed silica and diblock copolymer via mist modification, Prog. Org. Coat. 148 (2020), 105884, https://doi.org/10.1016/j.porgcoat.2020.105884.
[42] S. Naderizadeh, S. Dante, P. Picone, M. Di Carlo, R. Carzino, A. Athanassiou, I. S. Bayer, Bioresin-based superhydrophobic coatings with reduced bacterial adhesion, J. Colloid Interface Sci. 574 (2020) 20–32, https://doi.org/10.1016/j.jcis.2020.04.031.
[43] I. Torun, M. Ruzi, F. Er, M.S. Onses, Superhydrophobic coatings made from biocompatible polydimethylsiloxane and natural wax, Prog. Org. Coat. 136 (2019), 105279, https://doi.org/10.1016/j.porgcoat.2019.105279.
[44] T. Kim, H. Kang, N. Yoon, Synthesis of non-fluorinated paraffinic water repellents and application properties on textile fabrics, Fibers Polym. 18 (2017) 285–289, https://doi.org/10.1007/s12221-017-6469-4.
[45] C. Colleoni, E. Guido, V. Migani, G. Rosace, Hydrophobic behaviour of non-fluorinated sol–gel based cotton and polyester fabric coatings, J. Ind. Text. 44 (2015) 815–834, https://doi.org/10.1177/1528083713516664.
[46] T. Koussoulou, Photodegradation and photostabilization of historic silks in the museum environment – evaluation of a new conservation treatment., (n.d.) 14.
[47] Ö. Altun, N. Becenen, Antioxidant, Antibacterial and UV-Resistant Activities of Undyed and Dyed Wool Fabrics Treated with CuO Nanoparticles, J. Nanosci. Nanotechnol. 17 (2017) 4204–4209, https://doi.org/10.1166/jnn.2017.13119.
[48] Th.I. Shaheen, M.E. El-Naggar, A.M. Abdelgawad, A. Hebeish, Durable antibacterial and UV protections of in situ synthesized zinc oxide nanoparticles onto cotton fabrics, Int. J. Biol. Macromol. 83 (2016) 426–432, https://doi.org/10.1016/j.ijbiomac.2015.11.003.
[49] K. Hou, Y. Zeng, C. Zhou, J. Chen, X. Wen, S. Xu, J. Cheng, P. Pi, Facile generation of robust POSS-based superhydrophobic fabrics via thiol-ene click chemistry, Chem. Eng. J. 332 (2018) 150–159, https://doi.org/10.1016/j.cej.2017.09.074.
[50] M.M. Abd El-Hady, S. Sharaf, A. Farouk, Highly hydrophobic and UV protective properties of cotton fabric using layer by layer self-assembly technique, Cellulose. 27 (2020) 1099–1110, https://doi.org/10.1007/s10570-019-02815-0.
[51] M. Parhizkar, Y. Zhao, X. Wang, T. Lin, Photostability and durability properties of photochromic organosilica coating on fabric, J. Eng. Fiber. Fabr. 9 (2014), https://doi.org/10.1177/155892501400900308.
[52] S. Ayazi-Yazdi, L. Karimi, M. Mirjalili, M. Karimnejad, Fabrication of photochromic, hydrophobic, antibacterial, and ultraviolet-blocking cotton fabric using silica nanoparticles functionalized with a photochromic dye, J. Text. Inst. 108 (2017) 856–863, https://doi.org/10.1080/00405000.2016.1195088.
[53] T.V. Nguyen, P. Nguyen Tri, T.D. Nguyen, R. El Aidani, V.T. Trinh, C. Decker, Accelerated degradation of water borne acrylic nanocomposites used in outdoor protective coatings, Polym. Degrad. Stab. 128 (2016) 65–76, https://doi.org/10.1016/j.polymdegradstab.2016.03.002.
[54] O. Nechyporchuk, K. Kolman, M. Oriola, M. Persson, K. Holmberg, R. Bordes, Accelerated ageing of cotton canvas as a model for further consolidation practices, Journal of Cultural Heritage 28 (2017) 183–187, https://doi.org/10.1016/j.culher.2017.05.010.
[55] G. Mazzon, M. Zahid, J.A. Heredia-Guerrero, E. Balliana, E. Zendri, A. Athanassiou, I.S. Bayer, Hydrophobic treatment of woven cotton fabrics with polyurethane modified aminosilicone emulsions, Appl. Surf. Sci. (2019), https://doi.org/10.1016/j.apsusc.2019.06.069.
[56] M.Á. Bonet-Aracil, P. Díaz-García, E. Bou-Belda, N. Sebastiá, A. Montoro, R. Rodrigo, UV protection from cotton fabrics dyed with different tea extracts, Dye. Pigment. 134 (2016) 448–452, https://doi.org/10.1016/j.dyepig.2016.07.045.
[57] M. Shabbir, L.J. Rather, F. Mohammad, Economically viable UV-protective and antioxidant finishing of wool fabric dyed with Tagetes erecta flower extract: Valorization of marigold, Ind. Crops Prod. 119 (2018) 277–282, https://doi.org/10.1016/j.indcrop.2018.04.016.
[58] L.F. Zemljič, J. Volmajer, T. Ristić, M. Bracic, O. Sauperl, T. Kreže, Antimicrobial and antioxidant functionalization of viscose fabric using chitosan–curcumin formulations, Text. Res. J. 84 (2014) 819–830, https://doi.org/10.1177/0040517513512396.
[59] A.I. Quilez-Molina, J.A. Heredia-Guerrero, A. Armirotti, U.C. Paul, A. Athanassiou, I.S. Bayer, Comparison of physicochemical, mechanical and antioxidant properties of polyvinyl alcohol films containing green tealeaves waste extracts and discarded balsamic vinegar, Food Packag. Shelf Life 23 (2020), 100445, https://doi.org/10.1016/j.fpsl.2019.100445.
[60] A.I. Quilez-Molina, L. Marini, A. Athanassiou, I.S. Bayer, UV-blocking, transparent, and antioxidant polycyanoacrylate films, Polymers. 12 (2020) 2011, https://doi.org/10.3390/polym12092011.
[61] R. Johnston-Feller, Color science in the examination of museum objects: nondestructive procedures, Color Res. Appl. 27 (2002) 456–457, https://doi.org/10.1002/col.10107.
[62] E. Cappelletto, E. Callone, R. Campostrini, F. Girardi, S. Maggini, C. della Volpe, S. Siboni, R. Di Maggio, Hydrophobic siloxane paper coatings: the effect of increasing methyl substitution, J. Solgel Sci. Technol. 62 (2012) 441–452, https://doi.org/10.1007/s10971-012-2747-1.
[63] C.-H. Xue, S.-T. Jia, J. Zhang, L.-Q. Tian, Superhydrophobic surfaces on cotton textiles by complex coating of silica nanoparticles and hydrophobization, Thin Solid Films 517 (2009) 4593–4598, https://doi.org/10.1016/j.tsf.2009.03.185.
[64] V. Trovato, G. Rosace, C. Colleoni, S. Sfameni, V. Migani, M.R. Plutino, Sol-gel based coatings for the protection of cultural heritage textiles, IOP Conf. Ser.: Mater. Sci. Eng. 777 (2020), 012007, https://doi.org/10.1088/1757-899X/777/1/012007.
[65] N. Abidi, L. Cabrales, C.H. Haigler, Changes in the cell wall and cellulose content of developing cotton fibers investigated by FTIR spectroscopy, Carbohydr. Polym. 100 (2014) 9–16, https://doi.org/10.1016/j.carbpol.2013.01.074.
[66] P. Garside, P. Wyeth, Identification of cellulosic fibres by FTIR spectroscopy - thread and single fibre analysis by attenuated total reflectance, Stud. Conserv. 48 (2003) 269–275, https://doi.org/10.1179/sic.2003.48.4.269.
[67] M.K. Trivedi, A. Branton, D. Trivedi, G. Nayak, R. Singh, S. Jana, Physicochemical and spectroscopic characterization of biofield treated butylated hydroxytoluene, J. Food Ind. Microbiol. 1 (2015), https://doi.org/10.4172/jfim.1000101.
[68] T. Elzein, M. Nasser-Eddine, C. Delaite, S. Bistac, P. Dumas, FTIR study of polycaprolactone chain organization at interfaces, J. Colloid Interface Sci. 273 (2004) 381–387, https://doi.org/10.1016/j.jcis.2004.02.001.
[69] L. Ceseracciu, J.A. Heredia-Guerrero, S. Dante, A. Athanassiou, I.S. Bayer, Robust and biodegradable elastomers based on corn starch and polydimethylsiloxane (PDMS), ACS Appl. Mater. Interfaces 7 (2015) 3742–3753, https://doi.org/10.1021/am508515z.
[70] A. Boukir, I. Mehyaoui, S. Fellak, L. Asia, P. Doumenq, The effect of the natural degradation process on the cellulose structure of Moroccan hardwood fiber: a survey on spectroscopy and structural properties, Mediterr. J. Chem. 8 (2019) 179, https://doi.org/10.13171/10.13171/mjc8319050801ab.
[71] V. Librando, Z. Minniti, S. Lorusso, Ancient and modern paper characterization by FTIR and Micro-Raman spectroscopy, Conservat. Sci. Cult. Heritage. 11 (2011) 249–268, https://doi.org/10.6092/issn.1973-9494/2700.
[72] J.M. Cardamone, J.M. Gould, S.H. Gordon, Characterizing aged textile fibers by fourier transform infrared photoacoustic spectroscopy: part I: comparison of artificial and natural ageing in cotton, Text. Res. J. 57 (1987) 235–239, https://doi.org/10.1177/004051758705700408.
[73] J. Łojewska, P. Miśkowiec, T. Łojewski, L.M. Proniewicz, Cellulose oxidative and hydrolytic degradation: in situ FTIR approach, Polym. Degrad. Stab. 88 (2005) 512–520, https://doi.org/10.1016/j.polymdegradstab.2004.12.012.
[74] S. Sato, M. Suzuki, S. Kanehashi, K. Nagai, Permeability, diffusivity, and solubility of benzene vapor and water vapor in high free volume silicon- or fluorine-containing polymer membranes, J. Memb. Sci. 360 (2010) 352–362, https://doi.org/10.1016/j.memsci.2010.05.029.

[75] C. Kapridaki, P. Maravelaki-Kalaitzaki, TiO2–SiO2–PDMS nano-composite hydrophobic coating with self-cleaning properties for marble protection, Prog. Org. Coat. 76 (2013) 400–410, https://doi.org/10.1016/j.porgcoat.2012.10.006.
[76] H.F. Hoefnagels, D. Wu, G. de With, W. Ming, Biomimetic superhydrophobic and highly oleophobic cotton textiles, Langmuir. 23 (2007) 13158–13163, https://doi.org/10.1021/la702174x.
[77] M. Contardi, A. Alfaro-Pulido, P. Picone, S. Guzman-Puyol, L. Goldoni, J.J. Benítez, A. Heredia, M.J. Barthel, L. Ceseracciu, G. Cusimano, O.R. Brancato, M. Di Carlo, A. Athanassiou, J.A. Heredia-Guerrero, Low molecular weight ε-caprolactone-p-coumaric acid copolymers as potential biomaterials for skin regeneration applications, PLoS One 14 (2019), https://doi.org/10.1371/journal.pone.0214956.
[78] J.A. Heredia-Guerrero, L. Ceseracciu, S. Guzman-Puyol, U.C. Paul, A. Alfaro-Pulido, C. Grande, L. Vezzulli, T. Bandiera, R. Bertorelli, D. Russo, A. Athanassiou, I.S. Bayer, Antimicrobial, antioxidant, and waterproof RTV silicone-ethyl cellulose composites containing clove essential oil, Carbohydr. Polym. 192 (2018) 150–158, https://doi.org/10.1016/j.carbpol.2018.03.050.